A PORTABLE GAMMA CAMERA FOR RADIATION MONITORING *

S.V. Guru, Z. He, D.K. Wehe and G.F. Knoll
Department of Nuclear Engineering
The University of Michigan, Ann Arbor, MI 48109.

Abstract

A compact gamma camera capable of imaging high energy gamma rays (up to 2 MeV) is currently being developed for nuclear industrial applications. This camera uses a three inch square Position Sensitive Photomultiplier Tube (PSPMT) [Hamamatsu, R-2487-05] coupled to a NaI(Tl) scintillator. The incoming gamma ray direction is determined by a segmented collimator. The camera exhibits energy resolutions of 17% FWHM at 122 keV and 12% FWHM at 662 keV. With the collimator design used, an angular resolution at the source plane of 6° FWHM was measured for 412 keV. Images have been obtained using gamma ray sources up to 1 MeV using this system. The image reconstruction technique used is presented in detail. Corrections for the non-uniformities across the face of the PSPMT are implemented to improve the spatial and spectral information content in the final image.

I. INTRODUCTION

Nuclear industrial gamma ray imaging poses a set of imaging conditions different from nuclear medical imaging. Nuclear medical gamma cameras are designed for low-energy, low-intensity, high-resolution, near-field applications. A nuclear industrial gamma ray camera is designed for high-energy, high-intensity, moderate resolution and far field imaging applications.

We have designed a multiple hole collimator and have fabricated a multiple pixel nuclear industrial gamma camera. The first generation nuclear industrial gamma ray camera [1] developed in our laboratories displayed good spatial and energy resolution, but required lengthy data acquisition times due to its single channel operation. The multiple aperture design of the collimator used here reduces the data acquisition time of the imager.

*This work was supported under the U.S. Department of Energy, Robotics for Hazardous Environments, Grant No.DOE-FG02-86NE37969.

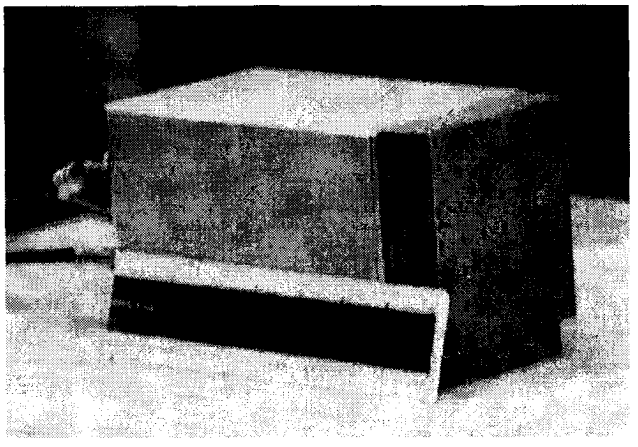

Figure 1: Photograph of the camera.

II. CAMERA DESIGN

Our objective is to build a high energy (up to 2 MeV) nuclear industrial gamma camera with a large field of view (Figure 1). Gamma cameras using PSPMTs have been fabricated and tested for nuclear medical applications [2]-[7] and nuclear industrial applications [8]-[11]. A collimator design was adopted after computer models indicated its effectiveness for our intended applications [12]. The direction of the incoming high energy gamma ray is defined by this multihole collimator (parallel hole, divergent collimator). This 5 × 5 collimator is fabricated out of a 2.54 cm thick block of machinable tungsten. The hole diameter is 0.20 cm and the septal thickness at the base of the collimator is 0.63 cm, giving a pitch of 0.83 cm and an opening angle of 9° for every hole. The axis of each hole is slanted 10° away from the axis of the neighboring hole. One hole was permanently blocked during the machining process.

A 7.5 cm × 7.5 cm × 1 cm NaI (Tl) crystal housed in a machined aluminum can with a 0.2 mm thick entrance window is used to detect the gamma rays passing through the collimator. All the inner faces of the scintillator are covered with a light-absorbing coating to minimize light spreading within the scintillator. The scintillation events

within the scintillator are read using the PSPMT. The PSPMT produces four outputs X1, X2, Y1 and Y2 from its resistive chains along the X and Y directions. Spatial coordinates of the interaction position are calculated using

$$X = (X1 - X2)/(X1 + X2) \quad (1)$$

$$Y = (Y1 - Y2)/(Y1 + Y2). \quad (2)$$

The energy deposited by a scintillation event (E) is the sum of the four outputs and is given by

$$E = X1 + X2 + Y1 + Y2. \quad (3)$$

A trigger and peak detection board was fabricated to read the peak values of the four outputs of the PSPMT. The sum of the four outputs (E) was used to trigger the four channel simultaneous analog to digital converter (ADC). Radiation Monitoring Devices (RMD) has fabricated a commercially available board which performs the above functions [13], and also has a software interface for data acquisition and for displaying real time images. The software reads the output of the PSPMT and performs a position estimation using Equations 1 and 2. From the estimated values of X and Y, a two dimensional map of the scintillation events within the scintillator is created (Figure 3).

Correction factors for variations in the gain across the face of the PSPMT are measured by flooding it with an isotropic source of known energy. The response of the PSPMT to this isotropic source is an indicator of the gain variations of the photocathode of the PSPMT. Calibration data gathered from this response is used by software to correct for non-uniformities when subsequent data acquisition is performed. The RMD board was used to acquire the images discussed in this paper.

III. Imaging Procedure

The collimator is designed to image hot, far-field sources. The holes are slanted such that the areas viewed by adjacent holes just intersect at an infinite distance away. With septal penetration, this this should work reasonably well for distant sources. For laboratory testing of nearby sources, this hole arrangement leads to incomplete sampling of the source plane. The holes of the collimator view discrete areas of the source plane (Figure 2) and there exist areas on the source plane that are not "visible" to the detector. For example, Figure 3 shows the image obtained from a continuous "M" shaped distributed source, and shows such regions. To image the "dead areas", the camera must be reoriented. The amount of total panning and tilting required is calculated from the source to camera distance. The total angular motion required (θ_{tilt}) by the camera to thoroughly sample the source plane is given by

$$\theta_{\text{tilt}} = \tan^{-1}\left[\left(\frac{2d+t}{h+a}\right) - \left(\frac{2d}{a} - \tan\theta_s\right)\right] \quad (4)$$

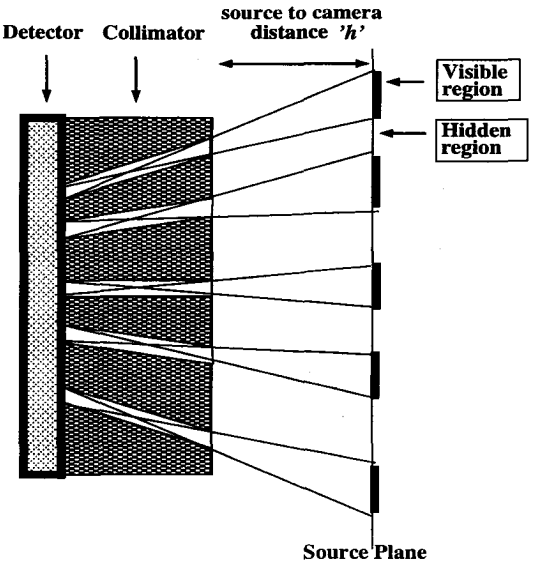

Collimator material: Tungsten
Collimator thickness (a) = 2.54 cm
Hole diameter (d) = 0.20 cm
Septal thickness (t) = 0.63 cm
Pitch (p) = d + t = 0.83 cm
Opening angle (θ) = 9°
Slant angle (θs) = 10°

Figure 2: Imaging technique of the camera

where:
h = distance between the source and the camera,
a = thickness of the collimator,
d = diameter of the holes of the collimator,
t = septal thickness of the collimator, and
θ_s = slant angle, the angle between the axis of neighbouring holes.
Note that as $h \gg (2d+t)$, $\theta_{\text{tilt}} \approx 0$.
The angular rotations are performed in steps not greater than the the opening angle of each hole ensuring a thorough sampling of the source plane with no 'dead areas'. The movement could also be performed in smaller steps resulting in a finer sampling of the image plane. For imaging sources located very close to the collimator relative to the parameters shown in Figure 2, Equation 4 showed that the camera had to be rotated by a total of 10°. If the source is located 10 cm away, for the same collimator, the camera has to be rotated by 5° to entirely sample the source plane.

In the prototype imager built, the relative motion between the source and the camera was introduced by moving the source relative to the camera. The prototype imager was fixed on the laboratory bench while the source distribution was located on a finely marked grid. The source was moved manually along the X and the Y axes to simulate panning and tilting of the camera. Each source position corresponds to a unique orientation of the camera. If the panning is performed in N_1 steps and the tilting

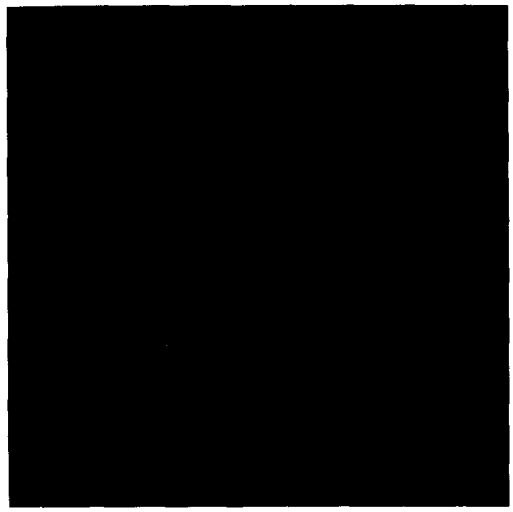

Figure 3: A typical gamma ray image of a continuous "M" shaped source distribution of ^{198}Au (412 keV), as seen on the detector plane. This image shows the shadow of the collimator expected from a single snap shot of the source plane.

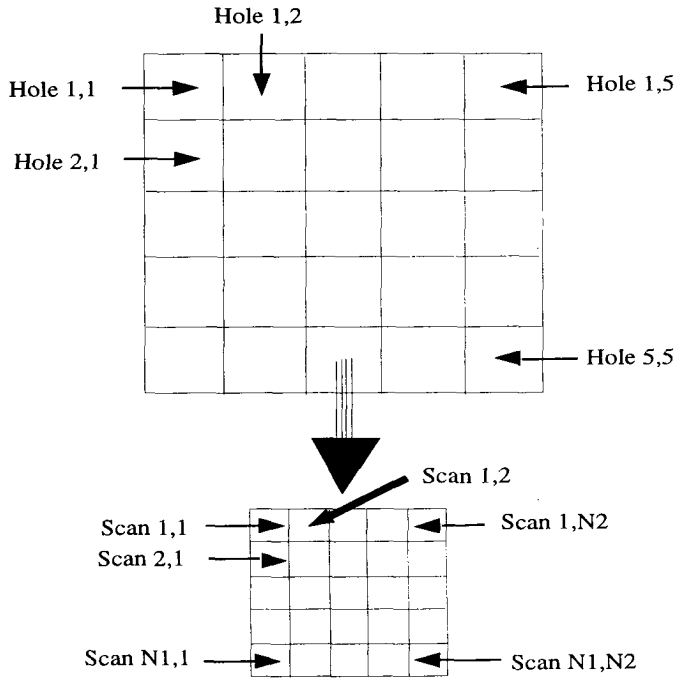

Figure 4: Image reconstruction procedure used in this camera

is performed in N_2 steps, then $N_1 \times N_2$ images from the camera are acquired.

A. *Image Reconstruction*

The image reconstruction technique is schematically represented in Figure 4, and is different from the reconstruction schemes adopted in nuclear medical gamma cameras. The method used here is a data integration technique. The image of the source plane obtained from the continuous crystal displays shadows of the collimator corresponding to the septal regions of the collimator. The data from the $N_1 \times N_2$ images must be integrated to yield the total image of the source plane. Since the collimator has an array of 5 × 5 holes, the entire source plane is subdivided into a matrix of 5 × 5 regions "seen" by the 25 holes of the collimator. Each element of this matrix is further subdivided into $N_1 \times N_2$ elements, corresponding to the $N_1 \times N_2$ images obtained by the camera. The full reconstructed image thus contains $(N_1 * 5) \times (N_2 * 5)$ pixels. A simple bilinear interpolation is applied to the 25 × 25 data values and yields the 512 × 512 images shown in Figures 5-7.

IV. Results

A. *Resolution*

The energy resolution of the camera depends upon the scintillator used. Narrowly collimated beams of 122 keV and 662 keV were incident on the scintillator and by measuring the sum of the four PSPMT outputs the energy resolution of the camera was measured. The energy resolution of the camera was measured to be 12% - 20% FWHM for ^{137}Cs (662 keV) gamma rays, and 17% - 23% for ^{57}Co (122 keV). This measurement was performed at various positions along the PSPMT face, giving rise to a range of values for the measured energy resolution.

The spatial resolution of the camera depends upon the thickness of the scintillator used. On the 1.0 cm thick NaI(Tl) crystal used in this camera, narrowly collimated beams of 122 keV and 662 keV were incident at known positions and the spread in the position estimation was measured to give the spatial resolution of the camera. The spatial resolution of the camera measured on the face of the PSPMT is 2.8 mm - 3.2 mm for 122 keV and 3.4 mm - 5.4 mm for 662 keV. This measurement was performed at various positions along the PSPMT face, giving rise to a range of values for the measured spatial resolution of the camera. These measurements are discussed in detail in [8].

The angular resolution of the camera depends on the nature of the collimator used in the camera. The collimator used here has a half opening angle of 4.5°. The angular resolution of the camera at the source plane was measured by taking a cross sectional slice of the image of the source plane (Figure 5). The angular resolution is calculated from known angular separation between the two vertical legs of the "U" shaped distribution. The angular resolution of the camera measured at the source plane is 6° FWHM for 412 keV. This measured value is consistent with the half opening angle of the holes of the collimator (4.5°).

The variation in the spatial and energy resolutions is

due primarily to the continuously varying gain across the PSPMT.

B. *Efficiency*

The efficiency of the camera is determined by both the efficiency of the collimator and the detection efficiency of the scintillator. The collimator efficiency is calculated to be $\approx 10^{-6}\%$ for a 1 MeV source at a distance of 1 meter on the axis of the collimator [12].

C. *Sensitivity*

The sensitivity of the camera, ξ, can be defined as the minimum activity required for a source to be detected significantly above the noise level of the camera. This is defined in terms of the signal to noise ratio as

$$\xi = \frac{N_{source} - N_{bkg}}{\sqrt{N_{bkg}}} \tag{5}$$

where ξ is the sensitivity, N_{source} is the total counts registered by the camera with a source present while N_{bkg} is the background registered by the camera. Both the source and the background are counted for the same duration. ξ signifies the difference of the measured total signal from the measured background counts in units of the standard deviation of the background counts. When ξ was measured at the camera center, with a 25 μCi gold point source (412 keV) located 30 cm away from the camera along the axis of the camera, and a counting time of 5000 sec, the signal to noise ratio of the image was measured to be 15. These sensitivity measurements were made for a single image. For ξ=5 and a counting time of one minute the camera is sensitive enough to detect a 80 μCi source of 412 keV located at a distance of 1 meter. This experimentally measured value of the sensitivity is in agreement with the theoretical value predicted during the design phase.

D. *Imaging*

Reconstructed images are shown in Figures 5-7. Figure 5 is an image of activated ^{198}Au wire shaped as a '**U**'. The vertical legs of the '**U**' measured 4.0 cm while the horizontal leg measured 5.5 cm. Figure 6 is an image of activated ^{198}Au wire shaped as an '**M**'. The vertical legs of the '**M**' measured 4.0 cm while the diagonal legs measured 3.8 cm. In both cases the $\sim$ 100 μCi source was located 10 cm away from the camera. The camera was panned and tilted 25 times to cover the entire source plane and produced 25 raw images to be combined. The raw images were obtained by counting for 25 seconds at each direction of the camera. The resultant image is a combination from the 25 raw images that were recorded. This image clearly shows the spatial distribution of the source in the

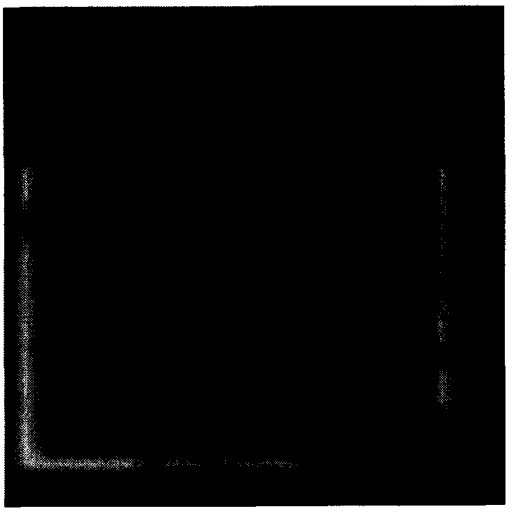

Figure 5: A reconstructed image of ^{198}Au '**U**' (412 keV) located 10 cm away

Figure 6: A reconstructed image of ^{198}Au '**M**' (412 keV) located 10 cm away

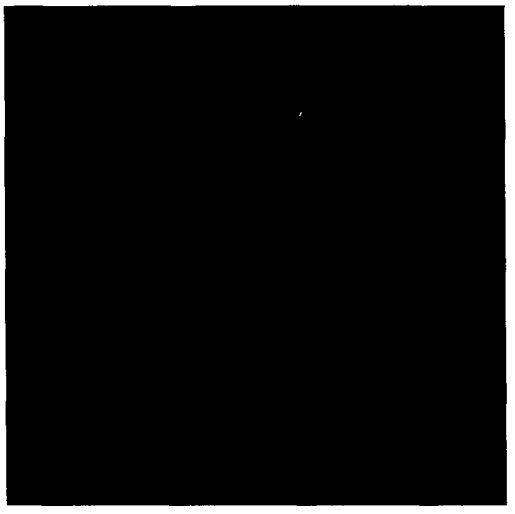

Figure 7: A reconstructed image of ^{58}Co point source (810 keV) located 10 cm away

source plane.[‡] The light shadows of the vertical legs in Figures 5 and 6 are caused by the difference between a planar translation of the source, and a true rotation of the camera. This effect is maximized for sources close to the collimator and at large angles relative to the central axis, which are conditions not of importance in the proposed applications. These shadow points have an intensity of $\sim$ 10% of the actual points and would disappear under a thresholding operation. Figure 7 is a reconstructed image of a source plane located 10 cm away from the camera containing a $\sim$ 100 μCi point source of ^{58}Co emitting 810 keV gamma rays.

E. *Spectrometry*

The energy sensitivity of the NaI(Tl) crystal allows this camera to be used as a spectrometer. Spectral analysis was performed and a hardware window was set on the data acquisition board, which enabled us to detect photons only within a chosen energy band. Hence the resultant images shown in Figures 3, 6-7 are distributions of a single selected energy in the source plane. This feature is particularly useful for rejecting scattered gamma rays from the environment and camera body.

V. Discussion

The data integration technique discussed in section III was applied successfully to the distributed 412 keV source and a point 810 keV source. These sources were chosen to demonstrate the ability of the camera to form images at these relatively high energies. One limitation in our procedure involved the assumption of the width of hole diameter at the detector plane. While the holes of the collimator have a diameter d, the effective hole diameter becomes larger due to septal penetration at higher energies. When the light spread within the crystal is also included the effective hole size increases further. In this work, the signals originating from the geometric area directly under the holes were treated as signals detected only through the open holes of the collimator. At higher energies (E $\geq$ 1 MeV) the signals originating within the area mapped by the effective hole diameter need to be considered.

[‡]The reconstructed image of the M shaped distribution shown in Figure 6 shows a dark area in the upper right hand corner although the source used was a continuous line source. This dark spot is attributed to one blocked hole in the collimator.

VI. Conclusion

A gamma camera was fabricated using a multiple hole collimator, NaI(Tl) crystal and PSPMT and tested at 412 keV and 810 keV. The images generated from this camera for close sources were presented and we expect improved performance for far-field sources. We are currently investigating means of extending the upper energy limit of this camera.

References

[1] T.A. DeVol, D.K. Wehe, and G.F. Knoll, "Gamma-ray spectral imaging using a single shutter radiation camera", *Nuclear Instruments and Methods*, vol. A299, pp. 495–500, 1990.

[2] N.J. Yasillo et al., "A single tube miniature gamma camera", Conference Record of 1993 IEEE NSS/MIC, 1994.

[3] Z. He, A.J. Bird, D. Ramsden, and Y. Meng, "A 5 inch diameter position-sensitive scintilation counter", *IEEE Transactions on Nuclear Science*, vol. 40, pp. 447–451, 1993.

[4] N.J. Yasillo, R.N. Beck, and M. Cooper, "Design considerations for a single tube gamma camera", *IEEE Transactions on Nuclear Science*, vol. 37, pp. 609–615, 1990.

[5] T.D. Milster et al., "A full-field modular gamma camera", *Journal of Nuclear Medicine*, vol. 31, pp. 632–639, 1990.

[6] M.V. Green et al., "Evaluation of cardiovascular function in small animals using a microcomputer-based scintigraphic imaging system", private communication, 1993.

[7] C.E. Ordonez, R.A. Mintzer, J.N. Aarsvold, N.J. Yasillo, and K.L. Mathews, "Simulation of imaging

with NaI(Tl) crystals and position sensitive photomultipilier tubes", *IEEE Transactions on Nuclear Science*, vol. 41, pp. 1510–1515, 1994.

[8] S.V. Guru, Z. He, J.C. Ferreira, D.K. Wehe, and G.F. Knoll, "A high energy gamma camera using a multiple hole collimator and PSPMT", *Nuclear Instruments and Methods*, vol. A353, pp. 328–333, 1994.

[9] R.H. Redus, M.R. Squillante, J. Gordon, D.K. Wehe, and G.F. Knoll, "A combined video and gamma ray imaging system for robots in nuclear environments", *Nuclear Instruments and Methods*, vol. A353, pp. 324–327, 1994.

[10] Z. He, A. Truman, S.V. Guru, D.K. Wehe, G.F. Knoll, and D. Ramsden, "Portable wide-angle γ-ray vision systems", this issue of the *Conference Proceedings.*

[11] R.H. Redus, V. Nagarkar, L.J. Cirignano, W. McGann, and M.R. Squillante, "A nuclear survey instrument with imaging capability", *IEEE Transactions on Nuclear Science*, vol. 33, pp. 1354–1357, 1992.

[12] S.V. Guru, J.D. Valentine, D.K. Wehe, and G.F. Knoll, "Monte Carlo modelling of a multiple-hole collimator for high energy gamma-ray imaging", *IEEE Transactions on Nuclear Science*, vol. 41, pp. 898–902, 1994.

[13] Radiation Monitoring Devices, "Position Sensitive Photomultiplier Interface System", private communication, 1993.